Structure and Madelung Energy of Coulomb Clusters

Hiroo Totsuji, Tokunari Kishimoto, Chieko Totsuji and Kenji Tsuruta

Graduate School of Natural Science and Technology and Faculty of Engineering, Okayama University, Tsushimanaka 3-1-1, Okayama 700-8530, Japan

Abstract. The ground state of the system of charged particles of one species confined by the three-dimensional, isotropic, and parabolic potential is investigated by molecular dynamics simulations. It is shown that, with the increase of the system size or the number of particles in the system N, the ground state changes from the shell-structured system to the finite bcc lattice with reconstructed surface. The critical value of the transition is estimated to be between $N = 10^4$ and $N = 2 \times 10^4$. The nucleation of the bcc lattice in the shell-structured cluster of 2×10^4 ions is observed.

INTRODUCTION

The systems of charges of one species confined in the external field provide us with a stage where various properties of strongly coupled plasmas manifest themselves in a simple and clear way. This system can be realized in the Penning-Malmberg [1]and Paul traps [2, 3] and direct experimental observations of these properties have been an excitement in recent years.

The ground state of these finite systems is strongly influenced by the geometry of confinement. When the external potential is the spherically symmetric parabola and the number of charges in the system is small, the structures such as icosahedron or spherical shells give the ground state. When the system has sufficiently large number of particles, it is expected that the ground state contains the bcc lattice as its main part: The ground state of the (infinite) one-component plasma is the bcc structure.

In experiments, the bcc lattice at the central part has been observed for large cloud of charges of the size more than 10^5 [4, 5]. The transition of the ground state from the shell structure to the bcc lattice has been expected to occur at the system size of 2×10^5 or larger [6]. It seems, however, that numerical simulations of larger systems may give more precise information related to this transition. The purpose of this paper is to compare the cohesive energy, sometimes called the Madelung energy, of these structures and show that the transition occurs between $N = 10^4$ and $N = 2 \times 10^4$ by molecular dynamics simulations of large clusters.

CP606, *Non-Neutral Plasma Physics IV*, edited by F. Anderegg et al.

PARAMETERS AND MADELUNG ENERGY

Let us here fix some notations for these clusters of charges. The Hamiltonian of our system H is given by $H = K + U$, where K is the kinetic energy

$$K = \sum_{i=1}^{N} \frac{1}{2} m \left(\frac{d\mathbf{r}_i}{dt} \right)^2, \tag{1}$$

and U, the potential energy

$$U = \sum_{i>j}^{N} \frac{q^2}{|\mathbf{r}_i - \mathbf{r}_j|} + \sum_{i=1}^{N} \frac{1}{2} k \mathbf{r}_i^2. \tag{2}$$

We define the Wigner-Seitz radius $a_{W\cdot S}$ by

$$a_{W\cdot S} = \left(\frac{q^2}{k} \right)^{1/3} \tag{3}$$

and rewrite K and U into the form

$$K = m \left(\frac{a_{W\cdot S}}{t_0} \right)^2 \sum_{i=1}^{N} \frac{1}{2} \left(\frac{d\mathbf{r}_i'}{dt'} \right)^2 \tag{4}$$

$$U = \left(\frac{q^2}{a_{W\cdot S}} \right) \left(\sum_{i>j}^{N} \frac{1}{|\mathbf{r}_i' - \mathbf{r}_j'|} + \sum_{i=1}^{N} \frac{1}{2} (\mathbf{r}_i')^2 \right). \tag{5}$$

Here the coordinates of particles are normalized by $a_{W\cdot S}$ and the time is normalized by t_0.

In the fluid approximation where charges are regarded as continuum, the ground state is the uniform distribution up to the radius R

$$R = \left(\frac{Nq^2}{k} \right)^{1/3} = N^{1/3} a_{W\cdot S} \tag{6}$$

with the density

$$n = \frac{3}{4\pi} \frac{k}{q^2}. \tag{7}$$

We note that $a_{W\cdot S}$ defined by (3) is the average mean distance or the ion-sphere radius in this approximation;

$$\frac{4\pi}{3} n a_{W\cdot S}^3 = 1. \tag{8}$$

The potential energy of the ground state in the fluid limit U_{homo} is given by

$$U_{homo} = \frac{3}{5} N^2 \frac{q^2}{R} + \frac{3}{10} N k R^2 = \frac{9}{10} N^{5/3} \frac{q^2}{a_{W\cdot S}}. \tag{9}$$

For given distribution of particles, we define the Madelung energy U_M by

$$U_M = U - U_{homo}. \tag{10}$$

At zero temperature, the behavior of the system is determined only by U. Therefore (5) indicates that our system is characterized by only one parameter, the system size N. At finite temperatures, we define the parameter Γ which represents the strength of the Coulomb coupling by

$$\Gamma = \frac{q^2}{k_B T a_{WS}}. \tag{11}$$

The static properties of the system at finite temperatures are characterized by the parameter Γ and the system size N.

In the fluid approximation, the radius of uniform distribution oscillates with the frequency

$$\omega_p = \left(\frac{3k}{m}\right)^{1/2} = \left(\frac{3q^2}{m a_{WS}^3}\right)^{1/2} = \left(\frac{4\pi q^2 n}{m}\right)^{1/2}. \tag{12}$$

This frequency characterizes the macroscopic evolution of our system. One of characteristic time scales of the microscopic evolution may be the time to move the mean distance by thermal velocity $a_{WS}/(k_B T/m)^{1/2}$ which is related to ω_p as

$$\omega_p \frac{a_{WS}}{(k_B T/m)^{1/2}} = (3\Gamma)^{1/2}. \tag{13}$$

NUMERICAL METHOD

Scaling with system size

We perform the molecular dynamics simulations. In this case, most of the computational time is consumed in the computation of the force on each particle and, with the naive method, the computational time increases rapidly in proportion to N^2 in our system where particles interact via the long-ranged Coulomb potential. We therefore adopt the fast multipole method [7] which enables one to perform molecular dynamics simulations of long-range force systems with the $O(N)$-scaling under controlled accuracy.

In the fast multipole method, the system is divided recursively into small cells and the interaction between particles belonging to well-separated cells is computed based on the multipole expansion and Taylor expansion. The number of smallest cells is 8^{level} and the level is adjusted so that the smallest cell has about 8 particles on the average [7]. For the system size of $N = 10^5$, we adopt the following parameters for the fast multipole method: the level of 5, multipole expansion up to 2^6-th order, the Taylor expansion up to 6th order, the well-separatedness of 2 (in the highest level, direct computation is applied for nearest and next-nearest neighbor cells). In the course of molecular dynamics simulation, the accuracy of the Madelung energy is kept at least for the first 4 digits and the direct computation is performed for final relaxed states. The parameters for smaller systems are also determined to give the accuracy at least of the same order.

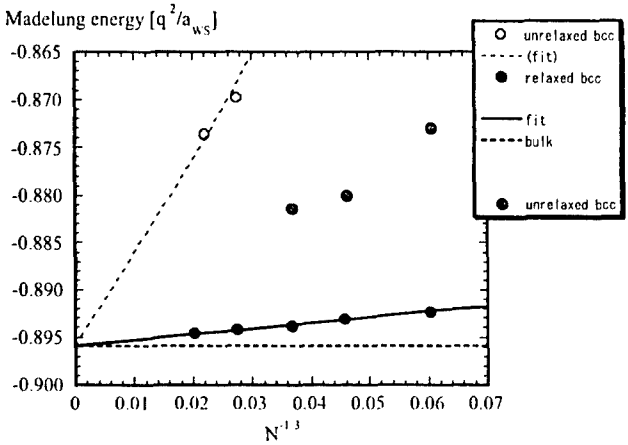

FIGURE 1. Madelung energy vs. system size for spherical bcc matter. Solid circles are the values with relaxed surface and solid line is the interpolation. Open and gray circles are examples of values without relaxation.

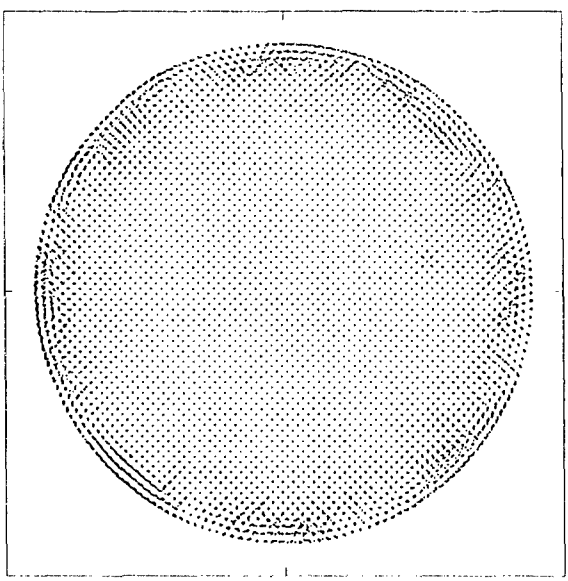

FIGURE 2. Particle distribution near the equatorial plane in spherical bcc matter with relaxed surface for $N = 120,032$. Positions of particles in the domain $|z| < 2.7a_{WS}$ are projected.

The temperature is controlled by the Nosé-Hoover method. In order to keep the homogeneity of the temperature, we attach multiple thermostats each controlling the kinetic energy of about 5000 particles.

Initial conditions

For the system of the size N, the radius of particle distribution in the fluid-limit ground state is determined as (6). The initial positions for the shell structure is given by the uniform random distribution of particles within this sphere. The velocities are given by the random distribution corresponding to the temperature specified by the value of Γ. After annealing with Γ values between 100 and 150 for sufficiently many steps in measures of the time scales (12) and (13), we slowly decrease the temperature.

Another set of initial conditions is the spherical cutout of the three-dimensional lattice and the random distribution of velocities. In this case, the value of Γ is kept just above the melting point (low temperature side) of the infinite lattice for a sufficiently long time to allow the system to relax before slowly increased.

MADELUNG ENERGY OF RELAXED SPHERICAL BCC MATTER

The spherical cutout of he bcc lattice has rather high surface energy as is shown in Fig. 1. When we anneal this system keeping the temperature near but below the melting point, we obtain the spherical bcc matter with reconstructed surface. The Madelung energy of the spherical bcc matter with reconstructed surface is also shown in Fig. 1 for the system sizes $N = 4544$, $10,464$, $20,288$, $48,928$, and $120,032$. We observe that the relaxation near the surface largely reduces the Madelung energy [8]. This is not expected from the high values of the Madelung energy of unrelaxed spherical bcc matter. An example of the structure is shown in Figs. 2 and 3. We observe that the relaxation has occurred within a few layers at the surface

In the limit of very large values of N, the Madelung energy may have the form

$$\frac{U_M}{Nq^2/a_{WS}} = E_\infty + \frac{E_s}{N^{1/3}}, \tag{14}$$

where the second term expresses the effect of the surface. When fitted to this form with E_∞ = -0.895929 (the Madelung energy of an infinite bcc solid), as shown in Fig. 1 by the solid line, we have $E_s = 0.0605$.

MADELUNG ENERGY OF SHELL-STRUCTURED SPHERICAL CLUSTERS

Starting from the random distribution in the sphere of radius R given by (6), we first anneal the system at the temperature above the melting temperature of bulk one-component

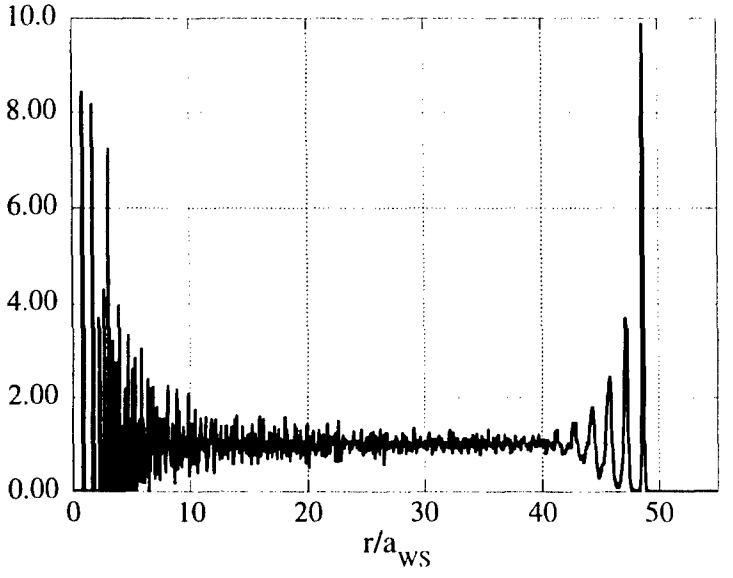

FIGURE 3. Radial distribution of particles in spherical bcc matter with relaxed surface for $N = 120,032$.

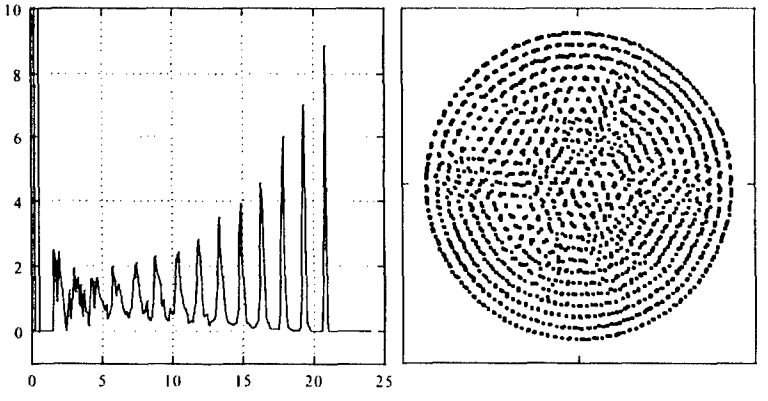

FIGURE 4. Particle distribution in shell-structured spherical cluster with $N = 10,000$ (left). Positions of particles near the equatorial plane with $|z| < 1.2a_{W\text{-}S}$ are projected (right).

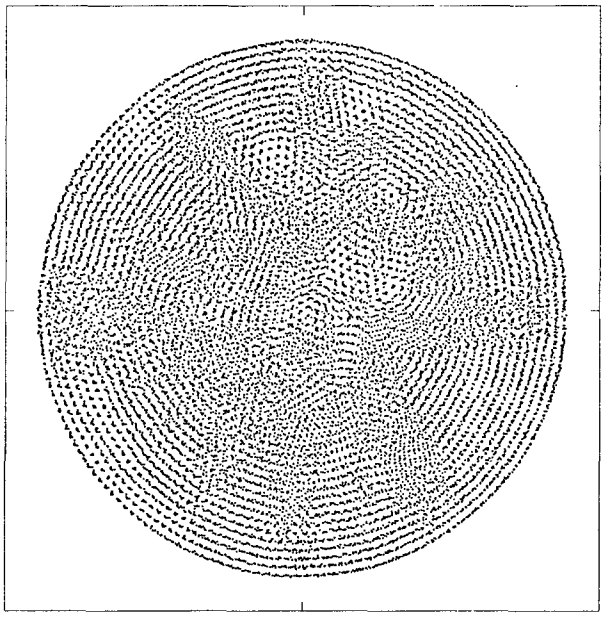

FIGURE 5. Particle distribution in shell-structured spherical cluster with $N = 100,000$.

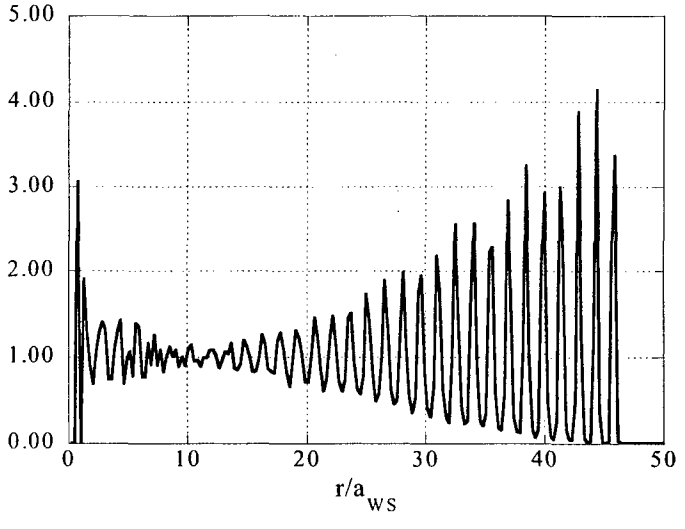

FIGURE 6. Projected positions of particles in the domain $|z| < 2.6a_{WS}$ for $N = 100,000$.

plasma. The typical value of Γ is around 100. We then slowly decrease the temperature of the system. The results are shown in Figs. 4, 5, and 6.

The values of the Madelung energy of the shell-structured spherical system of the size $N = 5 \times 10^3$, 10^4, 20288, and 10^5 are shown in Fig. 7. These values of the Medelung energy can be interpolated by the formula

$$\frac{U_M}{Nq^2/a_{WS}} = -0.8940 + 0.0219N^{-1/3}. \tag{15}$$

The largest simulated system in reports was $N = 2 \times 10^4$ [9].

TRANSITION OF THE GROUND STATE

The Madelung energies of the shell-structured clusters and of finite bcc matters with relaxed surface are compared in Fig. 7. We observe that, when the system size exceeds the critical value N_c, the ground state changes from the shell-structured cluster to the finite bcc lattice with relaxed surface. The critical system sized is given by the crossing of these Madelung energies and, in Fig. 7, is estimated to be around 10^4. We here note that these Madelung energy, especially of shell structures, could become lower by annealing the system repeatedly. The crossing, however, does not seem to be larger than 2×10^4. Taking into account this possibility, we here conclude that

$$10^4 < N_c < 2 \times 10^4. \tag{16}$$

NUCLEATION OF BCC LATTICE

The shell-structured cluster is still is a local minimum of the Madelung energy in the domain where $N > N_c$ and the bcc lattice with relaxed surface is the global minimum. Therefore it is not strange that the shell-structured cluster does not evolve to the bcc lattice with relaxed surface in simulations. One may, however, expect that there is a chance for the bcc lattice develops in the clusters of larger sizes. We here show one of such examples.

The distribution of particles near the equatorial plane of the cluster of $N = 20,288$ is shown in the left panel of Fig. 8. We observe that there exist a part where we have the structure with the straight planes rather than a curved plane in accordance with the surface. The structure factor for the particles in this domain is shown in the right panel of Fig. 8. We clearly see that the Bragg spots forms the fcc structure in the wave-number space. We have confirmed that the spacing between Bragg spots agree with those of the bcc lattice with the average density of this cluster. This domain thus forms the bcc lattice nucleated from the shell-structured cluster.

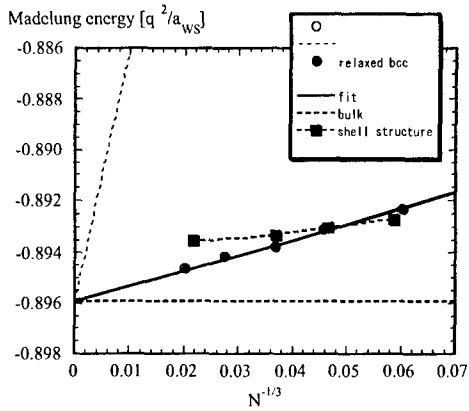

FIGURE 7. Madelung energy of spherical coulomb system vs. $N^{-1/3}$. Filled circles are relaxed spherical bcc matter and squares are shell structured systems.

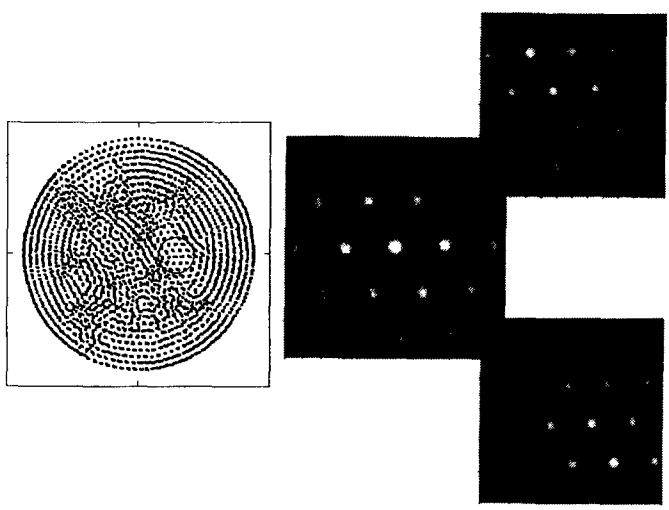

FIGURE 8. Bragg pattern from the central part (circled) of the shell-structured cluster of $N = 20,288$. Shown are consecutive three planes in reciprocal space where spots form the fcc lattice corresponding to bcc structure in real space.

CONCLUSIONS

It is shown that the ground state of the spherical coulomb clusters changes from shell-structured clusters to the finite bcc lattice with relaxed surface at the system size between 10^4 and 2×10^4. In the shell-structured cluster of 2×10^4, the nucleation of the bcc lattice is observed.

ACKNOWLEDGMENTS

This work has been partly supported by the Grants-in-Aid for Scientific Researches of the Ministry of Education, Culture, Sports, Science, and Technology of Japan, Nos. 08458109 and 11480110.

REFERENCES

1. Gilbert, S. L., Bollinger, J. J., and Wineland, D. J., Phys. Rev. Lett. **60**, 2022 (1988).
2. Birkl, G., Kassner, S., and Walther, H., Nature (London) **357**, 310 (1992).
3. Drewsen, M., Broderson, C., Hornekær, L. J., Hangst, S., and Schiffer, J. P., Phys. Rev. Lett. **81**, 2878 (1998).
4. Itano, W. M., Bollinger, J. J. , Tan, J. N., Jelenković, B., Huang, X. -P., and Wineland, D. J., Science **279**, 686 (1998).
5. Bollinger, J. J., Mitchell, T. B., Huang,X. -P., Itano, W. M., Tan, J. N., Jelenković, B., and Wineland, D. J., Phys. Plasmas, **7**, 7 (2000).
6. Dubin, D. H. E., and O'Neil, T. M., Rev. Mod. Phys. **71**, 87 (1999).
7. Greengard, L., and Rokhlin, V., J. Comput. Phys. **73**, 325 (1987).
8. Kishimoto, T., Totsuji, C., Tsuruta, K., and Totsuji, H., Physics Letters A **281**, 256 (2001).
9. Schiffer, J. P., *Non-Neutral Plasma Physics II*, edited by J. Fajans and D. H. E. Dubin, AIP Conference Proceedings 331, New York, 1995, p. 191.